
Information Geometry of Orthogonal Initializations and Training

Piotr A. Sokół

Department of Neurobiology and Behavior
Stony Brook University

Il Memming Park

Department of Neurobiology and Behavior
Department of Applied Mathematics and Statistics
Institute for Advanced Computational Sciences
Institute for AI-Driven Discovery and Innovation
Stony Brook University

Abstract

Recently mean field theory has been successfully used to analyze properties of wide, random neural networks. It has given rise to a prescriptive theory for initializing neural networks, which ensures that the ℓ_2 norm of the backpropagated gradients is bounded, and training is orders of magnitude faster. Despite the strong empirical performance of this class of initializations, the mechanisms by which they confer an advantage in the optimization of deep neural networks are poorly understood. Here we show a novel connection between the maximum curvature of the optimization landscape (gradient smoothness) as measured by the Fisher information matrix and the maximum singular value of the input-output Jacobian. Our theory partially explains why neural networks that are more isometric can train much faster. Furthermore, we experimentally investigate the benefits of maintaining orthogonality throughout training, from which we conclude that manifold constrained optimization of weights performs better regardless of the smoothness of the gradients. Finally we show that critical orthogonal initializations do not trivially give rise to a mean field limit of pre-activations for each layer.

1 INTRODUCTION

Deep neural networks (DNN) have shown tremendous success in computer vision problems, speech recognition, amortized probabilistic inference, and the modelling of

neural data. Despite their performance, DNNs face obstacles in their practical application, which stem from both the excessive computational cost of running gradient descent for a large number of epochs, as well as the inherent brittleness of gradient descent applied to very deep models. A number of heuristic approaches such as batch normalization, weight normalization and residual connections [15, 17, 29] have emerged in an attempt to address these trainability issues. Recently mean field theory has been successful in developing a more principled analysis of gradients of neural networks, and proposed a new random initialization principle. The mean field approach postulates that in the limit of wide layers and for random weight matrices with independently distributed entries the distribution of pre-activations converges weakly to an isotropic Gaussian. Using this approach, a series of works proposed to initialize the networks in such a way that for each layer the input-output Jacobian has mean singular values of 1 [32]. This requirement was further strengthened to suggest that the spectrum of singular values of the input-output Jacobian should concentrate on one, and that this can only be achieved with random orthogonal weight matrices. Under these conditions the back-propagated gradients are bounded in ℓ_2 norm [27], i.e. they neither vanish nor explode. It was shown experimentally in [10, 27, 36] that networks with these *critical* initial conditions train orders of magnitude faster than networks with arbitrary initializations.

This invites questions from an optimization perspective on how the spectrum of the hidden layer input-output Jacobian relates to notions of curvature of the parameters space, and hence convergence rate. The largest effective initial step size η_0 is proportional to $\frac{m}{M}$ for stochastic gradient descent, where the input-output Jacobian plays a central role for determining the local gradient smoothness M^\ddagger and the

[‡]Recall that the gradient smoothness M which will be of particular interest to us, is the Lipschitz constant of the gradients $\|\nabla f(x_1) - \nabla f(x_2)\| \leq M \|x_1 - x_2\|$, and for twice differentiable objectives, it is the maximum eigenvalue of the Hessian $\lambda_{max}(\nabla^2 f(x))$

(potentially negative) strong convexity m [8, 9]. Recent attempts have been made to analyze the mean field geometry of the optimization landscape using the Fisher information matrix (FIM) [3, 18], which given its close correspondence with the Hessian of the neural network defines an approximate gradient smoothness. Karakida et al. [18] derived an upper bound on the maximum eigenvalue in terms of the sum of the Frobenius norms of its constituent blocks. However, this bound is not satisfactory for critical initializations since by construction the mean square singular values of Jacobians of each layer are 1.

In this paper, we develop a new bound on the maximum eigenvalue of the Fisher information matrix $\lambda_{max}(\bar{\mathbf{G}})$ under critical initialization. It allows us to show that the maximum eigenvalue of the FIM is proportional to the maximum squared singular value of the hidden layer input-output Jacobian $s_{max}(\mathbf{J}_{\mathbf{x}^0}^{\mathbf{x}^L})$. With this we show that, paradoxically, critically initialized networks with a lower $s_{max}(\mathbf{J}_{\mathbf{x}^0}^{\mathbf{x}^L})$ and hence lower $\lambda_{max}(\bar{\mathbf{G}})$ train slower and attain a lower test accuracy. We experimentally demonstrate that it is due to a rapid increase of the latter, which limits the maximal stable step size via $\eta_t \leq \frac{m}{M} \approx \frac{m}{\lambda_{max}(\bar{\mathbf{G}})}$. We then investigate whether constraining the spectrum of the Jacobian matrix of each layer affects optimization rate. We do so by training networks using Riemannian optimization to constrain their weights to be orthogonal, or nearly orthogonal and we find that manifold constrained networks are insensitive to the distribution of $s_{max}(\mathbf{J}_{\mathbf{x}^0}^{\mathbf{x}^L})$ at the beginning of training unlike the unconstrained gradient descent (“Euclidean”). Furthermore, manifold constrained networks, unlike the Euclidean, minimize training loss rapidly, regardless of the local smoothness. In particular, we observe that the advantage conferred optimizing over manifolds cannot be explained by the improvement of the gradient smoothness as measured by $\lambda_{max}(\bar{\mathbf{G}})$, which argues against the proposed role of Batch Normalization recently put forward in [4, 30]. Importantly, Euclidean training with an appropriately chosen $s_{max}(\mathbf{J}_{\mathbf{x}^0}^{\mathbf{x}^L})$ reduce the test misclassification loss at approximately the same rate as their manifold constrained counterparts, and overall attain a higher accuracy. Finally, we show that for random networks with orthogonal weights, pre-activations do not necessarily converge in distribution to a Gaussian, raising questions about the conditions under which the mean field approximation holds.

2 Background

2.1 Formal Description of the Network

Following [27, 28, 32], we consider a feed-forward, fully connected neural network with L hidden layers. Each layer $l \in \{1, \dots, L\}$ is given as a recursion of the form

$$\mathbf{x}^l = \phi(\mathbf{h}^l), \quad \mathbf{h}^l = \mathbf{W}^l \mathbf{x}^{l-1} + \mathbf{b}^l \quad (1)$$

where \mathbf{x}^l are the activations, \mathbf{h}^l are the pre-activations, $\mathbf{W}^l \in \mathbb{R}^{N \times N}$ are the weight matrices, \mathbf{b}^l are the bias vectors and $\phi(\cdot)$ is the activation function. The input is denoted as \mathbf{x}^0 . The output layer of the network computes $\hat{\mathbf{y}} = g^{-1}(\mathbf{h}^g)$ where g is GLM a link function and $\mathbf{h}^g = \mathbf{W}^g \mathbf{x}^L + \mathbf{b}^g$.

The hidden layer input-output Jacobian matrix $\mathbf{J}_{\mathbf{x}^0}^{\mathbf{x}^L}$ is,

$$\mathbf{J}_{\mathbf{x}^0}^{\mathbf{x}^L} \triangleq \frac{\partial \mathbf{x}^L}{\partial \mathbf{x}^0} = \prod_{l=1}^L \mathbf{D}^l \mathbf{W}^l \quad (2)$$

where \mathbf{D}^l is a diagonal matrix with entries $\mathbf{D}_{i,i}^l = \phi'(\mathbf{h}_i^l)$. As pointed out in [27, 32], the conditioning of the Jacobian matrix affects the conditioning of the back-propagated gradients for all layers.

2.2 Critical Isometric Initializations

Extending the classic result on the Gaussian process limit for wide layer width obtained by Neal [25], recent work [21, 23] has shown that for deep untrained networks with elements of their weight matrices $\mathbf{W}_{i,j}$ drawn from a Gaussian distribution $\mathcal{N}(0, \frac{\sigma_{\mathbf{W}}^2}{N})$ the empirical distribution of the pre-activations \mathbf{h}^l converges weakly to a Gaussian distribution $\mathcal{N}(0, q^l \mathbf{I})$ for each layer l in the limit of the width $N \rightarrow \infty$. Under this mean-field condition, the variance of the pre-activation distribution q^l is recursively given by,

$$q^l = \sigma_{\mathbf{W}}^2 \int \phi(\sqrt{q^{l-1}} h) d\mu(h) + \sigma_{\mathbf{b}}^2 \quad (3)$$

where $\mu(h)$ denotes the standard Gaussian measure $\frac{dh}{\sqrt{2\pi}} \exp(-\frac{h^2}{2})$ and $\sigma_{\mathbf{b}}^2$ denotes the variance of the Gaussian distributed biases [32]. The variance of the pre-activations of the first layer q^1 depends on the ℓ_2^2 norm of the inputs $q^1 = \frac{\sigma_{\mathbf{W}}^2}{N} \|\mathbf{x}^0\|_2^2 + \sigma_{\mathbf{b}}^2$. The recursion defined in (3) has a fixed point q^* ,

$$q^* = \sigma_{\mathbf{W}}^2 \int \phi(\sqrt{q^*} h) d\mu(h) + \sigma_{\mathbf{b}}^2 \quad (4)$$

which can be satisfied for all layers by appropriately choosing $\sigma_{\mathbf{W}}$, $\sigma_{\mathbf{b}}$ and scaling the input \mathbf{x}^0 accordingly. Under this condition $\phi'(\mathbf{h}^l)$ for $1 \leq l \leq L$ are identically distributed. In order to ensure that $\mathbf{J}_{\mathbf{x}^0}^{\mathbf{x}^L}$ is well conditioned, Pennington et al. [27] require that in addition to the variance of pre-activation being constant for all layers, two additional constraints are met. Firstly, they require that the mean square singular value of $\mathbf{D}\mathbf{W}$ for each layer have a certain value in expectation.

$$\chi = \frac{1}{N} \mathbb{E}[\text{Tr}[(\mathbf{D}\mathbf{W})^\top \mathbf{D}\mathbf{W}]] = \sigma_{\mathbf{W}}^2 \int [\phi'(\sqrt{q^*} h)]^2 d\mu(h) \quad (5)$$

Given that the mean squared singular value of the Jacobian matrix $\mathbf{J}_{\mathbf{x}^0}^{\mathbf{x}^L}$ is $(\chi)^L$, they require that $\chi = 1$ which

corresponds to a critical initialization where the gradients are asymptotically stable as $L \rightarrow \infty$. Secondly, they require that the maximal squared singular value s_{max}^2 of the Jacobian $\mathbf{J}_{x^0}^{x^L}$ be bounded. In [27] it was shown that for weights with Gaussian distributed elements, the maximal singular value increases linearly in depth even if the network is initialized with $\chi = 1$. Fortunately, for orthogonal weights, the maximal singular value s_{max} is bounded even as $L \rightarrow \infty$ [28] and for piecewise-linear $\phi(\cdot)$, it is analytically derivable and admits a solution in q^* for $s_{max}(\mathbf{J}_{x^0}^{x^L}) = 1$ for any choice of L . For arbitrary $\phi(\cdot)$'s, s_{max} can be obtained numerically from the solution of a functional equation describing the density of singular values [27]. Because orthogonal weight matrices are necessary for the hidden layer input-output Jacobian matrix to act as near isometry, we restrict our attention for the remainder of the paper to only this class of critical initializations. It is also important to note that while orthogonal initializations can preserve the ℓ_2 norm across arbitrary numbers of layers, they break the mean field assumption that the elements of \mathbf{W} are independently and identically distributed. We discuss the implication of this violation in 3.5.

3 Results

3.1 Establishing a Connection Between the Jacobian and Fisher Information Matrix

To better understand the geometry of the optimization landscape, we wish to put a Lipschitz bound on the gradient. Thus our goal is to express it using the results of the previous section. As presented below, we noticed that by using the Fisher information matrix (FIM), we can derive analytically an approximation to the Lipschitz bound, because FIM is a quadratic form of Jacobian matrices with respect to parameters.

In particular, for the class of critical, orthogonal initializations, we want to express the expected maximum eigenvalue of a random Fisher information matrix in terms of the expected maximum singular value of the Jacobian $\mathbf{J}_{x^0}^{x^L}$. To do so, let us consider the output of a multilayer perceptron as defining a conditional probability distribution $p_\theta(\mathbf{y}|\mathbf{x}^0)$, where $\Theta = \{\text{vec}(\mathbf{W}^1), \dots, \text{vec}(\mathbf{W}^L), \mathbf{b}^1, \dots, \mathbf{b}^L\}$ is the set of all hidden layer parameters, and θ is the column vector containing the concatenation of all the parameters in Θ . In this context, the Fisher information matrix is defined as [2, 7, 22],

$$\bar{\mathbf{G}} \triangleq \mathbb{E}_{\mathbf{x}^0, \mathbf{y}} [\nabla_\theta \log p_\theta(\mathbf{y}|\mathbf{x}^0) \nabla_\theta \log p_\theta(\mathbf{y}|\mathbf{x}^0)^\top] \quad (6)$$

which can be expanding using the chain rule:

$$\bar{\mathbf{G}} = \mathbb{E}_{\mathbf{x}^0, \mathbf{y}} \left[\mathbf{J}_\theta^{x^L \top} \mathbf{W}^{g \top} \nabla_{\mathbf{h}^g} \log p_\theta(\mathbf{y}|\mathbf{x}^0) \nabla_{\mathbf{h}^g} \log p_\theta(\mathbf{y}|\mathbf{x}^0)^\top \mathbf{W}^g \mathbf{J}_\theta^{x^L} \right]. \quad (7)$$

Each block of the Fisher information matrix with respect to parameters $a, b \in \Theta$ can further be expressed as

$$\bar{\mathbf{G}}_{a,b} = \mathbb{E}_{\mathbf{x}^0} \left[\mathbf{J}_a^{h^\alpha \top} \mathbf{J}_{h^\alpha}^{x^L \top} \mathbf{W}^{g \top} \mathbf{H}_g \mathbf{W}^g \mathbf{J}_{h^\beta}^{x^L} \mathbf{J}_b^{h^\beta} \right] \quad (8)$$

where the final layer Hessian \mathbf{H}_g is defined as $\nabla_{\mathbf{h}^g}^2 \log p_\theta(\mathbf{y}|\mathbf{x}^0)$. We can re-express the outer product of the score function $\nabla_{\mathbf{h}^g} \log p_\theta(\mathbf{y}|\mathbf{x}^0)$ as the second derivative of the log-likelihood, provided it is twice differentiable and it does not depend on \mathbf{y} , which also allows us to drop \mathbf{y} from the expectation. This condition naturally holds for all canonical link functions and matching generalized linear model loss functions. We define the matrix of partial derivatives of the α -th layer pre-activations with respect to the layer specific parameters separately for \mathbf{W}^α and \mathbf{b}^α as:

$$\mathbf{J}_a^{h^\alpha} = \mathbf{x}^{\alpha-1 \top} \otimes \mathbf{I} \quad \text{for } a = \text{vec}(\mathbf{W}^\alpha) \quad (9)$$

$$\mathbf{J}_a^{h^\alpha} = \mathbf{I} \quad \text{for } a = \mathbf{b}^\alpha \quad (10)$$

We can further simplify the expression for the blocks of the Fisher information matrix (8), using the fact that the pre-activations converge weakly to an isotropic Gaussian distribution with mean zero and variance q^* in the limit of wide layers [21, 23]. This justifies assuming independence of the pre-activations of all the layers. We can additionally assume for convenience that the input to the network \mathbf{x}^0 has been whitened before being scaled by $\sqrt{q^*}$. The simplified expressions are as follows:

$$\begin{aligned} \bar{\mathbf{G}}_{\text{vec}(\mathbf{W}^\alpha), \text{vec}(\mathbf{W}^\beta)} &= \mathbb{E} \left[\mathbf{x}^{\alpha-1} \mathbf{x}^{\beta-1 \top} \otimes \mathbf{J}_{h^\alpha}^{x^L \top} \mathbf{W}^{g \top} \mathbf{H}_g \mathbf{W}^g \mathbf{J}_{h^\beta}^{x^L} \right] \\ &= \mathbb{E} \left[\mathbf{x}^{\alpha-1} \mathbf{x}^{\beta-1 \top} \right] \otimes \mathbb{E} \left[\mathbf{J}_{h^\alpha}^{x^L \top} \mathbf{W}^{g \top} \mathbf{H}_g \mathbf{W}^g \mathbf{J}_{h^\beta}^{x^L} \right] \quad (11) \end{aligned}$$

Note that the expectation is also over the random networks realizations [3]. By the assumed independence of the elements of $\mathbf{h}^{\alpha-1}$ and $\mathbf{h}^{\beta-1}$, the covariance is zero for all pairs $\alpha \neq \beta$. For the α -block diagonal elements of the FIM, the expectation becomes

$$\begin{aligned} \mathbb{E} \left[\mathbf{x}^{\alpha-1} \mathbf{x}^{\alpha-1 \top} \right] &= \\ \mathbb{E}_{h \sim \mathcal{N}(0, \sqrt{q^*})} \left[(\phi(h) - \mathbb{E}_{h \sim \mathcal{N}(0, \sqrt{q^*})} [\phi(h)])^2 \right] \mathbf{I} \quad (12) \end{aligned}$$

The variance is constant for all elements of the vector $\mathbf{x}^{\alpha-1}$ again by independence of the elements of $\mathbf{h}^{\alpha-1}$. This quantity can either be evaluated directly by computing the variance analytically or by approximating using the delta method. For the sake of clarity, we restrict further derivation to $\phi(\cdot) = \tanh(\cdot)$, for which the delta method yields,

$$\mathbb{E} \left[\mathbf{x}^{\alpha-1} \mathbf{x}^{\alpha-1 \top} \right] \approx (\phi'(0))^2 q^* \mathbf{I} = q^* \mathbf{I} \quad (13)$$

The blocks with respect to biases are given as

$$\bar{\mathbf{G}}_{\mathbf{b}^\alpha, \mathbf{b}^\beta} = \mathbb{E} \left[\mathbf{J}_{h^\alpha}^{x^L \top} \mathbf{W}^{g \top} \mathbf{H}_g \mathbf{W}^g \mathbf{J}_{h^\beta}^{x^L} \right] \quad (14)$$

and the blocks with respect to both weights and biases are given as

$$\bar{\mathbf{G}}_{\text{vec}(\mathbf{W}^\alpha), \mathbf{b}^\beta} = \mathbb{E}[\mathbf{x}^{\alpha-1\top} \otimes \mathbf{I}] \mathbb{E}[\mathbf{J}_{\mathbf{h}^\alpha}^{x^L\top} \mathbf{W}^{g\top} \mathbf{H}_g \mathbf{W}^g \mathbf{J}_{\mathbf{h}^\beta}^{x^L}] \quad (15)$$

For odd activation functions $\phi(\cdot)$, such as \tanh considered by Pennington et al. [27], the leftmost expectation is zero.

We then consider a block diagonal approximation to the Fisher information matrix. Under this simplification, the maximum eigenvalue of the the Fisher information matrix is $\lambda_{\max}(\bar{\mathbf{G}}) \approx \max_a \lambda_{\max}(\bar{\mathbf{G}}_{a,a})$. To justify the quality of this approximation we use the Gershgorin circle theorem for block-partitioned matrices, detailed in Appendix A.2. Following (11) the spectral norm of each diagonal block a with respect to the weight matrices \mathbf{W}^α is bounded above by $q^* s_{\max}^2(\mathbf{J}_{\mathbf{h}^\alpha}^{x^L}) s_{\max}^2(\mathbf{W}^g) \lambda_{\max}(\mathbf{H}_g)$, while the diagonal blocks a with respect to the biases \mathbf{b}^α are bounded by $s_{\max}^2(\mathbf{J}_{\mathbf{h}^\alpha}^{x^L}) s_{\max}^2(\mathbf{W}^g) \lambda_{\max}(\mathbf{H}_g)$ using (14). These results can be further simplified if we initialize \mathbf{W}^g as a scaled semi-orthogonal matrix such that $\mathbf{W}^{g\top} \mathbf{W}^g = \sigma_{\mathbf{W}}^2 \mathbf{I}$ which implies,

$$s_{\max}(\mathbf{J}_{\mathbf{h}^\alpha}^{x^L}) = \frac{1}{\sigma_{\mathbf{W}}} s_{\max}(\mathbf{J}_{\mathbf{x}^\alpha}^{x^L}) \quad (16)$$

because the spectral norm is unitarily invariant and absolutely homogeneous. This simplifies the previous expressions to

$$\lambda_{\max}(\bar{\mathbf{G}})_{\text{vec}(\mathbf{W}^\alpha), \text{vec}(\mathbf{W}^\alpha)} = q^* s_{\max}^2(\mathbf{J}_{\mathbf{x}^\alpha}^{x^L}) \lambda_{\max}(\mathbf{H}_g) \\ \lambda_{\max}(\bar{\mathbf{G}})_{\mathbf{b}^\alpha, \mathbf{b}^\alpha} = s_{\max}^2(\mathbf{J}_{\mathbf{x}^\alpha}^{x^L}) \lambda_{\max}(\mathbf{H}_g)$$

Based on analytic results [27] and the empirical observations in [28] that the maximum singular values of the Jacobian are monotonically increasing as depth increases, we assume $s_{\max}(\mathbf{J}_{\mathbf{h}^\alpha}^{x^L})$ is a monotonically increasing function of $(L - \alpha)$. It is therefore sufficient to consider the blocks associated with the bottom layer. Then, $\lambda_{\max}(\bar{\mathbf{G}})$ is approximately $\lambda_{\max}(\bar{\mathbf{G}})_{\mathbf{b}^1, \mathbf{b}^1}$ if $q^* < 1$ or $\lambda_{\max}(\bar{\mathbf{G}})_{\text{vec}(\mathbf{W}^1), \text{vec}(\mathbf{W}^1)}$ otherwise. This result shows that the strong smoothness, given by the maximum eigenvalue of the FIM, is proportional to the squared maximum singular value of the input-output Jacobian. This in turn implies that as $s_{\max}(\mathbf{J}_{\mathbf{x}^0}^{x^L})$ increases, gradient smoothness deteriorates and the maximum admissible initial step size decreases.

3.2 Optimization over manifolds

Optimizing neural network weights subject to manifold constraints has recently attracted considerable interest [5, 11, 12, 16, 26, 34, 38]. In this work we probe how constraining the weights of each layer to be orthogonal or near orthogonal affects the spectrum of the hidden layer input-output Jacobian and of the Fisher information matrix.

We briefly review notions from differential geometry and optimization over matrix manifolds [1, 13], in order to lay ground for a discussion of the specifics of the optimization techniques used in our experiments. Informed readers are encouraged to skip to Sec. 3.2.1. The potentially non-convex constraint set constitutes a Riemannian manifold, when it is locally isomorphic to \mathbb{R}^n , differentiable and endowed with a suitable (Riemannian) metric, which allows us to measure distances in the tangent space and consequently also define distances on the manifold. There is considerable freedom in choosing a Riemannian metric; here we consider the metric inherited from the Euclidean embedding space which is defined as $\langle \mathbf{W}, \mathbf{W}' \rangle \triangleq \text{Tr}(\mathbf{W}'^\top \mathbf{W})$.

Stiefel Manifold Let $\text{St}(p, n)$ ($p \leq n$) denote the set of all $n \times p$ orthonormal matrices

$$\text{St}(p, n) \triangleq \{\mathbf{W} \in \mathbb{R}^{n \times p} : \mathbf{W}^\top \mathbf{W} = \mathbf{I}_p\} \quad (17)$$

Notice that for $p = n$, the Stiefel manifold parametrizes the set of all orthogonal matrices.

Oblique Manifold Let $\text{Ob}(p, n)$ denote the set of all $n \times p$ matrices with unit norm columns

$$\text{Ob}(p, n) \triangleq \{\mathbf{W} \in \mathbb{R}^{n \times p} : \text{diag}(\mathbf{W}^\top \mathbf{W}) = \mathbf{1}\} \quad (18)$$

where $\text{diag}(\mathbf{M})$ denotes an operator that extracts the diagonal entries of \mathbf{M} . Constraining the weights to this manifold is equivalent to using Weight Normalization [29].

To optimize a cost function with respect to parameters lying in a non-Euclidean manifold we must define a descent direction. This is done by defining a manifold equivalent of the directional derivative. An intuitive approach replaces the movement along a vector \mathbf{t} with movement along a geodesic curve $\gamma(t)$, which lies in the manifold and connects two points $\mathbf{W}, \mathbf{W}' \in \mathcal{M}$ such that $\gamma(0) = \mathbf{W}$, $\gamma(1) = \mathbf{W}'$. The derivative of an arbitrary smooth function $f(\gamma(t))$ with respect to t then defines a tangent vector for each t .

Tangent vector $\xi_{\mathbf{W}}$ is a tangent vector at \mathbf{W} if $\xi_{\mathbf{W}}$ satisfies $\gamma(0) = \mathbf{W}$ and

$$\xi_{\mathbf{W}} \triangleq \left. \frac{df(\gamma(t))}{dt} \right|_{t=0} \triangleq \gamma'(0) f \quad (19)$$

The set of all tangents to \mathcal{M} at \mathbf{W} is referred to as the tangent space to \mathcal{M} at \mathbf{W} and is denoted by $T_{\mathbf{W}}\mathcal{M}$. The geodesic importantly is then specified by a constant velocity curve $\gamma''(t) = 0$ with initial velocity $\xi_{\mathbf{W}}$. To perform a gradient step, we must then move along $\xi_{\mathbf{W}}$ while respecting the manifold constraint. This is achieved by applying the exponential map defined as $\text{Exp}_{\mathbf{W}}(\xi_{\mathbf{W}}) \triangleq \gamma(1)$, which moves \mathbf{W} to another point \mathbf{W}' along the geodesic. While

certain manifolds, such as the Oblique manifold, have efficient closed-form exponential maps, for general Riemannian manifolds, the computation of the exponential map involves numerical solution to a non-linear ordinary differential equation [1]. An efficient alternative to numerical integration is given by an orthogonal projection onto the manifold. This projection is formally referred to as a retraction $\text{Rt}_{\mathbf{W}} : T_{\mathbf{W}}\mathcal{M} \rightarrow \mathcal{M}$.

Finally, gradient methods using Polyak (heavy ball) momentum (e.g. ADAM [19]) require the iterative updating of terms which naturally lie in the tangent space. The parallel translation $\mathcal{T}_{\zeta}(\xi) : T\mathcal{M} \oplus T\mathcal{M} \rightarrow T\mathcal{M}$ generalizes vector composition from Euclidean to non-Euclidean manifolds, by moving the tangent ξ along the geodesic with initial velocity $\zeta \in \mathcal{T}$ and endpoint \mathbf{W}' , and then projecting the resulting vector onto the tangent space $T_{\mathbf{W}'}\mathcal{M}$. As with the exponential map, parallel transport \mathcal{T} may require the solution of non-linear ordinary differential equation. To alleviate the computational burden, we consider *vector transport* as an effective, projection-like solution to the parallel translation problem. We overload the notation and also denote it as \mathcal{T} , highlighting the similar role that the two mappings share. Technically, the geodesics and consequentially the exponential map, retraction as well as transport \mathcal{T} depend on the choice of the Riemannian metric. Putting the equations together the updating scheme for Riemannian stochastic gradient descent on the manifold is

$$\mathbf{W}_{t+1} = \Pi_{\mathbf{W}_t}(-\eta_t \text{grad}f) \quad (20)$$

where Π is either the exponential map Exp or the retraction Rt and $\text{grad}f$ is the gradient of the function $f(\mathbf{W})$ lying in the tangent space $T_{\mathbf{W}}\mathcal{M}$.

3.2.1 Optimizing over the Oblique manifold

Cho and Lee [11] proposed an updating scheme for optimizing neural networks where the weights of each layer are constrained to lie in the oblique manifold $\text{Ob}(p, n)$. Using the fact that the manifold itself is a product of p unit-norm spherical manifolds, they derived an efficient, closed-form Riemannian gradient descent updating scheme. In particular the optimization simplifies to the optimization over $\text{Ob}(1, n)$ for each column $\mathbf{w}_{i \in \{1, \dots, p\}}$ of \mathbf{W} .

Oblique gradient The gradient $\text{grad}f$ of the cost function f with respect to the weights lying in $\text{Ob}(1, n)$ is given as a projection of the Euclidean gradient $\text{Grad}f$ onto the tangent at \mathbf{w}

$$\text{grad}f = \text{Grad}f - (\mathbf{w}^\top \text{Grad}f)\mathbf{w} \quad (21)$$

Oblique exponential map The exponential map $\text{Exp}_{\mathbf{w}}$ moving \mathbf{w} to \mathbf{w}' along a geodesic with initial velocity $\xi_{\mathbf{w}}$

$$\text{Exp}_{\mathbf{w}} = \xi_{\mathbf{w}} \cos(\|\mathbf{w}\|) + \frac{\mathbf{w}}{\|\mathbf{w}\|} \sin(\|\mathbf{w}\|) \quad (22)$$

Oblique parallel translation The parallel translation \mathcal{T} moves the tangent vector $\xi_{\mathbf{w}}$ along the geodesic with initial velocity $\zeta_{\mathbf{w}}$

$$\begin{aligned} \mathcal{T}_{\zeta_{\mathbf{w}}}(\xi_{\mathbf{w}}) &= \xi_{\mathbf{w}} - \\ &\frac{\zeta_{\mathbf{w}}}{\|\zeta_{\mathbf{w}}\|} ((1 - \cos(\|\zeta_{\mathbf{w}}\|)) + \mathbf{w} \sin(\|\zeta_{\mathbf{w}}\|)) \frac{\zeta_{\mathbf{w}}}{\|\zeta_{\mathbf{w}}\|}^\top \xi_{\mathbf{w}} \end{aligned} \quad (23)$$

Cho and Lee [11] derived a regularization term which penalizes the distance between the point in the manifold \mathbf{W} and the closest orthogonal matrix with respect to the Frobenius norm.

$$\rho(\lambda, \mathbf{W}) = \frac{\lambda}{2} \|\mathbf{W}^\top \mathbf{W} - \mathbf{I}\|_F^2 \quad (24)$$

3.2.2 Optimizing over the Stiefel manifold

Optimization over Stiefel manifolds in the context of neural networks has been studied by [14, 34, 35]. Unlike [34, 35] we propose the parametrization using the Euclidean metric, which results in a different definition of vector transport.

Stiefel gradient The gradient $\text{grad}f$ of the cost function f with respect to the weights lying in $\text{St}(p, n)$ is given as a projection of the Euclidean gradient $\text{Grad}f$ onto the tangent at \mathbf{W} [1, 13]

$$\begin{aligned} \text{grad}f &= (\mathbf{I} - \mathbf{W}\mathbf{W}^\top)\text{Grad}f \\ &+ \frac{1}{2}\mathbf{W}(\mathbf{W}^\top \text{Grad}f - \text{Grad}f^\top \mathbf{W}) \end{aligned} \quad (25)$$

Stiefel retraction The retraction $\text{Rt}_{\mathbf{W}}(\xi_{\mathbf{W}})$ for the Stiefel manifold is given by the Q factor of the QR decomposition [1].

$$\text{Rt}_{\mathbf{W}}(\xi_{\mathbf{W}}) = \text{qf}(\mathbf{W} + \xi_{\mathbf{W}}) \quad (26)$$

Stiefel vector transport The vector transport \mathcal{T} moves the tangent vector $\xi_{\mathbf{w}}$ along the geodesic with initial velocity $\zeta_{\mathbf{w}}$ for $\mathbf{W} \in \text{St}(p, n)$ endowed with the Euclidean metric.

$$\mathcal{T}_{\zeta_{\mathbf{w}}}(\xi_{\mathbf{w}}) = (\mathbf{I} - \mathbf{Y}\mathbf{Y}^\top)\xi_{\mathbf{w}} + \frac{1}{2}\mathbf{Y}(\mathbf{Y}^\top \xi_{\mathbf{w}} - \xi_{\mathbf{w}}^\top \mathbf{Y}) \quad (27)$$

where $\mathbf{Y} \triangleq \text{Rt}_{\mathbf{W}}(\zeta_{\mathbf{W}})$. It is easy to see that the transport \mathcal{T} consists of a retraction of tangent $\zeta_{\mathbf{W}}$ followed by the orthogonal projection of $\eta_{\mathbf{W}}$ at $\text{Rt}_{\mathbf{W}}(\zeta_{\mathbf{W}})$. The projection is the same as the one mapping $\text{P} : \text{Grad}f \rightarrow \text{grad}f$ in (25).

3.3 Optimizing over non-compact manifolds

The critical weight initialization yielding a singular spectrum of the Jacobian tightly concentrating on 1 implies that a substantial fraction of the pre-activations lie in expectation in the linear regime of the squashing nonlinearity and

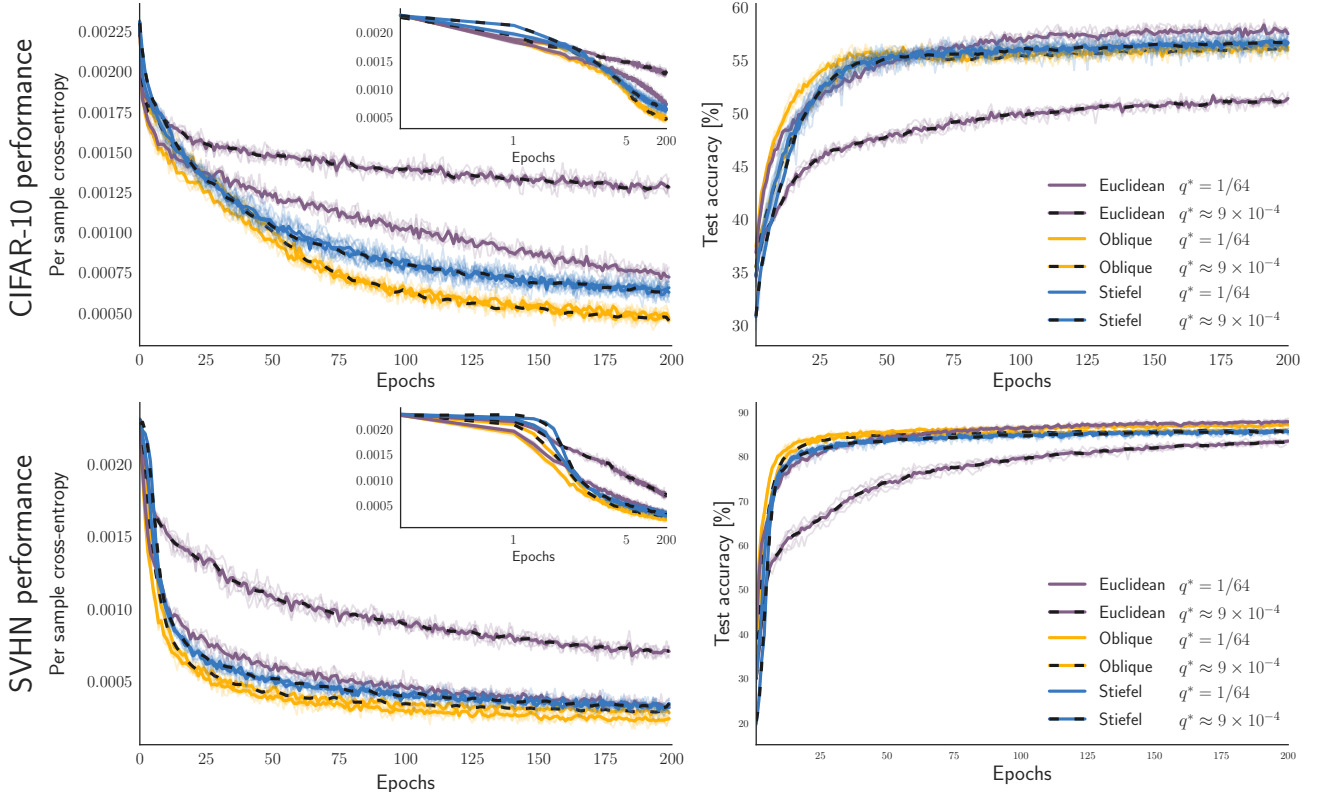


Figure 1: **Manifold constrained networks are insensitive to the choice of q^*** : Train loss and test accuracy for Euclidean, Stiefel and Oblique networks with two different values of q^* . The manifold constrained networks minimize the training loss at approximately the same rate, being faster than both Euclidean networks. Despite this, there is little difference between the test accuracy of the Stiefel and Oblique networks and the Euclidean networks initialized with $q^* = 9 \times 10^{-4}$. Notably, the latter attains a marginally higher test set accuracy towards the end of training.

as a consequence the network acts quasi-linearly. To relax this constraint during training we allow the scales of the manifold constrained weights to vary. We chose to represent the weights as a product of a scaling diagonal matrix and a matrix belonging to the manifold. Then the optimization of each layer consists in the optimization of the two variables in the product. In this work we only consider isotropic scalings, but the method generalizes easily to the use of any invertible square matrix.

3.4 Numerical Experiments

To experimentally test the potential effect of maintaining orthogonality throughout training and compare it to the unconstrained optimization [27], we trained a 200 layer tanh network on CIFAR-10 and SVHN. Following [27] we set the width of each layer to be $N = 400$ and chose the $\sigma_{\mathbf{W}}$, $\sigma_{\mathbf{b}}$ in such a way to ensure that χ concentrates on 1 but s_{max}^2 varies as a function of q^* (see Fig. 2). We considered two different critical initializations with $q^* = \frac{1}{64}$ and $q^* \approx 9 \times 10^{-4}$, which differ both in spread of the singular values as well as in the resulting training speed and final test accuracy as reported by [27]. To test how enforcing

strict orthogonality or near orthogonality affects convergence speed and the maximum eigenvalues of the Fisher information matrix, we trained Stiefel and Oblique constrained networks and compared them to the unconstrained “Euclidean” network described in [27]. We used a Riemannian version of ADAM [19]. When performing gradient descent on non-Euclidean manifolds, we split the variables into three groups: (1) Euclidean variables (e.g. the weights of the classifier layer, biases), (2) non-negative scaling $\sigma_{\mathbf{W}}$ both optimized using the regular version of ADAM, and (3) manifold variables optimized using Riemannian ADAM. The initial learning rates for all the groups, as well as the non-orthogonality penalty (see 24) for Oblique networks were chosen via Bayesian optimization, maximizing validation set accuracy after 50 epochs. All networks were trained with a minibatch size of 1000. We trained 5 networks of each kind, and collected eigenvalue and singular value statistics every 5 epochs, from the first to the fiftieth, and then after the hundredth and two hundredth epochs.

Based on the bound on the maximum eigenvalue of the Fisher information matrix derived in Section 3.1, we predicted that at initialization $\lambda_{max}(\hat{\mathbf{G}})$ should covary with

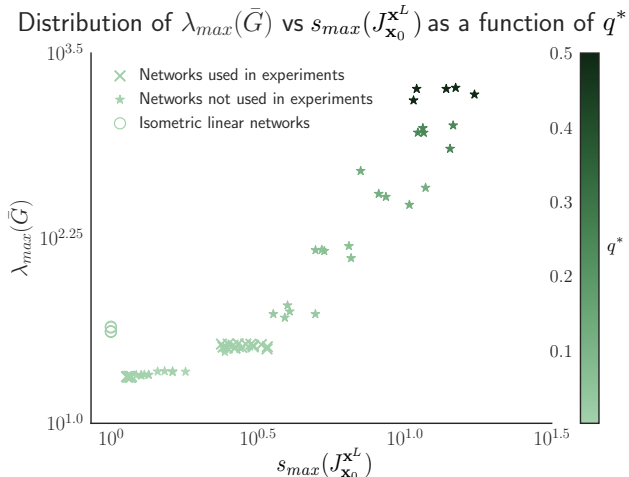


Figure 2: **At initialization the maximum eigenvalue of the Fisher information matrix \bar{G} correlates highly with the maximum singular value of the Jacobian $J_{x_0}^{x^L}$.**

$\sigma_{max}^2(J_{x_0}^{x^L})$. Our prediction is vindicated in that we find a strong, significant correlation between the two (Pearson coefficient $\rho = 0.88$). The numerical values are presented in Fig. 2. Additionally we see that both the maximum singular value and maximum eigenvalue increase monotonically as a function of q^* . Motivated by the previous work by Saxe et al. [31] showing depth independent learning dynamics in linear orthogonal networks, we included 5 instantiations of this model in the comparison. The input to the linear network was normalized the same way as the critical, non-linear networks with $q^* = 1/64$. The deep linear networks had a substantially larger $\lambda_{max}(\bar{G})$ than its non-linear counterparts initialized with identically scaled input (Fig. 2).

Having established a connection between q^* the maximum singular value of the hidden layer input-output Jacobian and the maximum eigenvalue of the Fisher information, we investigate the effects of initialization on subsequent optimization. As reported by Pennington et al. [27], the learning speed and generalization peak at intermediate values of $q^* \approx 10^{-0.5}$. This result is counterintuitive given that the maximum eigenvalue of the Fisher information matrix, much like that of the Hessian in convex optimization, upper bounds the maximal learning rate [8, 9]. To gain insight into the effects of the choice of q^* on the convergence rate, we trained the Euclidean networks and estimated the local values of λ_{max} during optimization. At the same time we asked whether we can effectively control the two afore-said quantities by constraining the weights of each layer to be orthogonal or near orthogonal. To this end we trained Stiefel and Oblique networks and recorded the same statistics.

We present training results in Fig. 1, where it can be seen that Euclidean networks with $q^* \approx 9 \times 10^{-4}$ per-

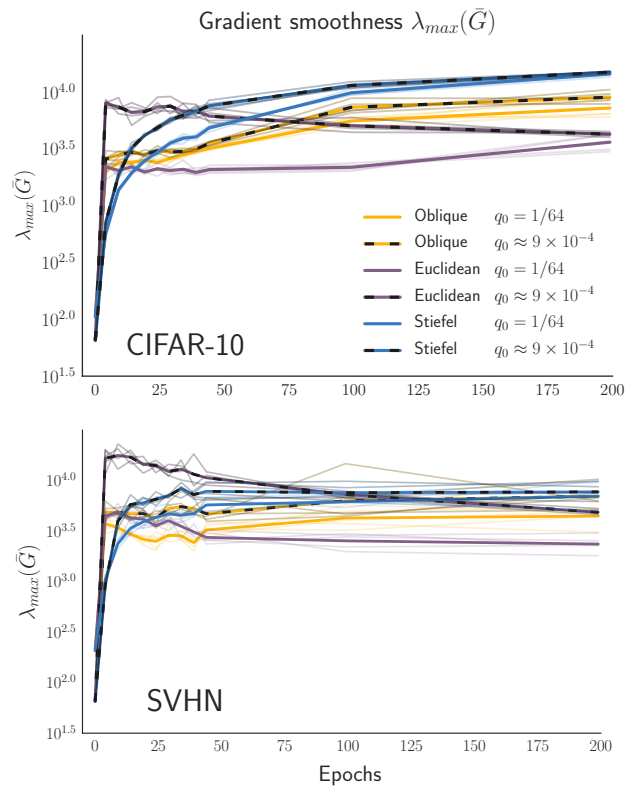


Figure 3: **For manifold constrained networks, gradient smoothness is not predictive of optimization rate. Euclidean networks with a low initial $\lambda_{max}(\bar{G})$ rapidly become less smooth, whereas Euclidean networks with a larger $\lambda_{max}(\bar{G})$ remain relatively smoother.** Notably, the Euclidean network with $q^* = 1/64$ has almost an order of magnitude smaller $\lambda_{max}(\bar{G})$ than the Stiefel and Oblique networks, but reduces training loss at a slower rate.

form worse with respect to training loss and test accuracy than those initialized with $q^* = 1/64$. On the other hand, manifold constrained networks are insensitive to the choice of q^* . Moreover, Stiefel and Oblique networks perform marginally worse on the test set compared to the Euclidean network with $q^* = 1/64$, despite attaining a lower training loss. This latter fact indicates that manifold constrained networks are perhaps prone to overfitting.

We observe that reduced performance of Euclidean networks initialized with $q^* \approx 9 \times 10^{-4}$ may partially be explained by their rapid increase in $\lambda_{max}(\bar{G})$ within the initial 5 epochs of optimization (see Fig. 3). While all networks undergo this rapid increase, it is most pronounced for Euclidean networks with $q^* \approx 9 \times 10^{-4}$. The increase $\lambda_{max}(\bar{G})$ correlates with the inflection point in the training loss curve that can be seen in the inset of Fig. 1. Interestingly, the manifold constrained networks optimize efficiently despite differences in $\lambda_{max}(\bar{G})$, showing that their performance cannot be attributed to increasing the gradient smoothness as postulated by [30].

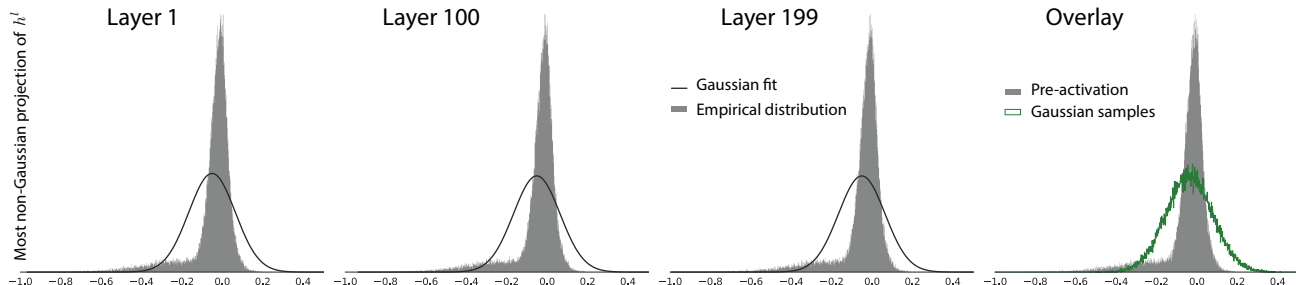


Figure 4: **Pre-activations for random networks $q^* = 1/64$ evaluated on CIFAR-10 contain a non-Gaussian subspace.** The projection was obtained using the algorithm in [6]. The rightmost panel shows an overlay of the pre-activations (all on top of each other) compared to the most non-Gaussian projection of a set of 400 dimensional Gaussian random variables with variance matched to the real data as control (green). Note that since the pre-activations are in the linear regime of tanh, and the weights are initialized to be orthogonal, the non-Gaussian component is expected to propagate through the layers.

3.5 Non-Gaussian limit of pre-activation

The derivation of the spectra of hidden layer input-output Jacobians presented in [27, 28] crucially depends on the existence of the Gaussian limit of the distribution of pre-activations, which in turn assumes that the elements of the weight matrices are sampled iid from some probability measure with finite first two moments. This condition is trivially violated for matrices sampled from the Haar (uniform) measure over the Stiefel manifold. We invoke Theorem 1 from Meckes [24] which asserts that for a random semi-orthogonal projection of an arbitrary random vector to converge to a Gaussian distribution in the bounded Lipschitz distance, the projection must go from d input dimensions to at most $\frac{2 \log(d)}{\log(\log(d))}$ dimensions. We also show empirically that in orthogonally initialized random networks, the pre-activations do not necessarily converge to a multivariate Gaussian distribution (see Fig. 4).

4 Discussion

Critical orthogonal initializations have proven tremendously successful in rapidly training very deep neural networks [10, 27, 28, 37]. Despite their elegant derivation drawing on methods from free probability and mean field theory, they did not offer a clear optimization perspective on the mechanisms driving their success. With this work we complement the understanding of critical orthogonal initializations by showing that the maximum eigenvalue of the Fisher information matrix, and consequentially the local gradient smoothness is proportional to the maximum singular value of the input-output Jacobian. This gives an information geometric account of why the step size and training speed depend on q^* via its effect on $s_{max}(\mathbf{J}_{\mathbf{x}^0}^L)$. We observed in numerical experiments that the paradoxical results reported in [27] whereby training speed and generalization attains a maximum for $q^* = 10^{-0.5}$ can potentially

be explained by a rapid increase of the maximum eigenvalue of the FIM during training for the networks initialized with Jacobians closer to being isometric (i.e., smaller q^*). This increase effectively limits the learning rate during the early phase of optimization. Moreover, we compared manifold constrained networks with the Euclidean network, each evaluated with two initial values of q^* . From these experiments we draw the conclusion that manifold constrained networks are less sensitive to the initial strong smoothness, unlike their Euclidean counterparts. Furthermore, we observe that the rate at which Stiefel and Oblique networks decrease training loss is not dependent on their gradient smoothness, a result which is consistent with the recent analysis of [20]. Although the random matrix predictions derived by [27, 28] closely match their experimental data, the mean field assumption does not hold, as seen in Fig. 4 and implied by the theorem in A.1. Understanding the exact conditions under which the mean field conditions hold, will qualify the conditions under which critical, orthogonal initializations will continue to facilitate the fast training of very deep neural networks.

References

- [1] Absil, P.-A., Mahony, R., and Sepulchre, R. (2007). *Optimization Algorithms on Matrix Manifolds*. Princeton University Press, Princeton, N.J. ; Woodstock.
- [2] Amari, S.-i. (2016). *Information Geometry and Its Applications*. Springer, Japan, 1st ed. 2016 edition edition.
- [3] Amari, S.-i., Karakida, R., and Oizumi, M. (2018). Fisher Information and Natural Gradient Learning of Random Deep Networks. *arXiv:1808.07172 [cond-mat, stat]*. arXiv: 1808.07172.
- [4] Anonymous (2018). A Mean Field Theory of Batch Normalization.
- [5] Arjovsky, M., Shah, A., and Bengio, Y. (2015).

- Unitary Evolution Recurrent Neural Networks. *arXiv:1511.06464 [cs]*. 00012 arXiv: 1511.06464.
- [6] Blanchard, G., Kawanabe, M., Sugiyama, M., Spokoiny, V., and Müller, K.-R. (2006). In Search of Non-Gaussian Components of a High-Dimensional Distribution. *Journal of Machine Learning Research*, 7(Feb):247–282.
- [7] Botev, A., Ritter, H., and Barber, D. (2017). Practical Gauss-Newton Optimisation for Deep Learning. In *International Conference on Machine Learning*, pages 557–565.
- [8] Bottou, L., Curtis, F. E., and Nocedal, J. (2016). Optimization Methods for Large-Scale Machine Learning. *arXiv:1606.04838 [cs, math, stat]*. arXiv: 1606.04838.
- [9] Boyd, S. and Vandenberghe, L. (2004). *Convex Optimization, With Corrections 2008*. Cambridge University Press, Cambridge, UK ; New York, 1 edition edition.
- [10] Chen, M., Pennington, J., and Schoenholz, S. (2018). Dynamical Isometry and a Mean Field Theory of RNNs: Gating Enables Signal Propagation in Recurrent Neural Networks. In *International Conference on Machine Learning*, pages 873–882.
- [11] Cho, M. and Lee, J. (2017). Riemannian approach to batch normalization. In *Advances in Neural Information Processing Systems*, pages 5229–5239.
- [12] Cisse, M., Bojanowski, P., Grave, E., Dauphin, Y., and Usunier, N. (2017). Parseval Networks: Improving Robustness to Adversarial Examples. *arXiv:1704.08847 [cs, stat]*. arXiv: 1704.08847.
- [13] Edelman, A., Arias, T. A., and Smith, S. T. (1998). The Geometry of Algorithms with Orthogonality Constraints. *SIAM Journal on Matrix Analysis and Applications*, 20(2):303–353.
- [14] Harandi, M. and Fernando, B. (2016). Generalized BackPropagation, \’{E}tude De Cas: Orthogonality. *arXiv:1611.05927 [cs]*. 00004 arXiv: 1611.05927.
- [15] He, K., Zhang, X., Ren, S., and Sun, J. (2015). Deep Residual Learning for Image Recognition. *arXiv:1512.03385 [cs]*. 01528 arXiv: 1512.03385.
- [16] Henaff, M., Szlam, A., and LeCun, Y. (2016). Recurrent Orthogonal Networks and Long-Memory Tasks. *arXiv:1602.06662 [cs, stat]*. arXiv: 1602.06662.
- [17] Ioffe, S. and Szegedy, C. (2015). Batch Normalization: Accelerating Deep Network Training by Reducing Internal Covariate Shift. *arXiv:1502.03167 [cs]*. 00385 arXiv: 1502.03167.
- [18] Karakida, R., Akaho, S., and Amari, S.-i. (2018). Universal Statistics of Fisher Information in Deep Neural Networks: Mean Field Approach. *arXiv:1806.01316 [cond-mat, stat]*. arXiv: 1806.01316.
- [19] Kingma, D. P. and Ba, J. (2014). Adam: A Method for Stochastic Optimization. *arXiv:1412.6980 [cs]*. 01869 arXiv: 1412.6980.
- [20] Kohler, J., Daneshmand, H., Lucchi, A., Zhou, M., Neymeyr, K., and Hofmann, T. (2018). Towards a Theoretical Understanding of Batch Normalization. *arXiv:1805.10694 [cs, stat]*. arXiv: 1805.10694.
- [21] Lee, J., Bahri, Y., Novak, R., Schoenholz, S. S., Pennington, J., and Sohl-Dickstein, J. (2017). Deep Neural Networks as Gaussian Processes. *arXiv:1711.00165 [cs, stat]*. arXiv: 1711.00165.
- [22] Martens, J. and Grosse, R. (2015). Optimizing Neural Networks with Kronecker-factored Approximate Curvature. *arXiv:1503.05671 [cs, stat]*. arXiv: 1503.05671.
- [23] Matthews, A. G. d. G., Rowland, M., Hron, J., Turner, R. E., and Ghahramani, Z. (2018). Gaussian Process Behaviour in Wide Deep Neural Networks. *arXiv:1804.11271 [cs, stat]*. arXiv: 1804.11271.
- [24] Meckes, E. (2012). Projections of Probability Distributions: A Measure-Theoretic Dvoretzky Theorem. In *Geometric Aspects of Functional Analysis*, Lecture Notes in Mathematics, pages 317–326. Springer, Berlin, Heidelberg.
- [25] Neal, R. M. (1996). *Bayesian Learning for Neural Networks*, volume 118 of *Lecture Notes in Statistics*. Springer New York, New York, NY.
- [26] Ozay, M. and Okatani, T. (2016). Optimization on Submanifolds of Convolution Kernels in CNNs. *arXiv preprint arXiv:1610.07008*. 00003.
- [27] Pennington, J., Schoenholz, S., and Ganguli, S. (2017). Resurrecting the sigmoid in deep learning through dynamical isometry: theory and practice. *Advances in neural information processing systems*.
- [28] Pennington, J., Schoenholz, S. S., and Ganguli, S. (2018). The Emergence of Spectral Universality in Deep Networks. *arXiv:1802.09979 [cs, stat]*. arXiv: 1802.09979.
- [29] Salimans, T. and Kingma, D. P. (2016). Weight Normalization: A Simple Reparameterization to Accelerate Training of Deep Neural Networks. *arXiv:1602.07868 [cs]*. 00003 arXiv: 1602.07868.
- [30] Santurkar, S., Tsipras, D., Ilyas, A., and Madry, A. (2018). How Does Batch Normalization Help Optimization? (No, It Is Not About Internal Covariate Shift). *arXiv:1805.11604 [cs, stat]*. arXiv: 1805.11604.
- [31] Saxe, A. M., McClelland, J. L., and Ganguli, S. (2013). Exact solutions to the nonlinear dynamics of learning in deep linear neural networks. *arXiv preprint arXiv:1312.6120*. 00083.
- [32] Schoenholz, S. S., Gilmer, J., Ganguli, S., and Sohl-Dickstein, J. (2016). Deep Information Propagation. *arXiv:1611.01232 [cs, stat]*. 00003 arXiv: 1611.01232.

- [33] Tretter, C. (2008). *Spectral Theory of Block Operator Matrices and Applications*. IMPERIAL COLLEGE PRESS.
- [34] Vorontsov, E., Trabelsi, C., Kadoury, S., and Pal, C. (2017). On orthogonality and learning recurrent networks with long term dependencies. *arXiv:1702.00071 [cs]*. arXiv: 1702.00071.
- [35] Wisdom, S., Powers, T., Hershey, J. R., Roux, J. L., and Atlas, L. (2016). Full-Capacity Unitary Recurrent Neural Networks. *arXiv:1611.00035 [cs, stat]*. arXiv: 1611.00035.
- [36] Xiao, L., Bahri, Y., Sohl-Dickstein, J., Schoenholz, S., and Pennington, J. (2018a). Dynamical Isometry and a Mean Field Theory of CNNs: How to Train 10,000-Layer Vanilla Convolutional Neural Networks. In *International Conference on Machine Learning*, pages 5393–5402.
- [37] Xiao, L., Bahri, Y., Sohl-Dickstein, J., Schoenholz, S. S., and Pennington, J. (2018b). Dynamical Isometry and a Mean Field Theory of CNNs: How to Train 10,000-Layer Vanilla Convolutional Neural Networks. *arXiv:1806.05393 [cs, stat]*. arXiv: 1806.05393.
- [38] Xie, D., Xiong, J., and Pu, S. (2017). All You Need is Beyond a Good Init: Exploring Better Solution for Training Extremely Deep Convolutional Neural Networks with Orthonormality and Modulation. *arXiv:1703.01827 [cs]*. arXiv: 1703.01827.

A Appendix

A.1 A measure Theoretic Condition for Convergence of Pre-activations to a Gaussian Distribution

Theorem 1 (Meckes [24]). *Let x be a random vector in \mathbb{R}^d with $\mathbb{E}[\|x\|^2] = \sigma^2 d$, $\mathbb{E}[\|x\|^2 \sigma^{-2} - d] \leq L\sqrt{d}$, and $\sup_{\xi \in \mathbb{S}^{d-1}} \mathbb{E}[(\xi^\top x)^2] \leq 1$. Let $x_{\mathbf{W}}$ denote the projection $\mathbf{W}x$ for $\mathbf{W} \in \text{St}(k, d)$, with $k = \delta \frac{\log(d)}{\log(\log(d))}$ and $0 \leq \delta \leq 2$, then there is a $c > 0$ such that for $\epsilon = 2 \exp\left[-c \frac{\log(\log(d))}{\delta}\right]$ there exists a subset $\mathfrak{J} \subseteq \text{St}(k, d)$ with probability mass $\mu(\mathfrak{J})$ with respect to the Haar measure μ over the manifold. Then $\mu(\mathfrak{J}) \geq 1 - C \exp(-c' d \epsilon^2)$ such that for all $\mathbf{W} \in \mathfrak{J}$,*

$$\sup_{\max(\|f\|_\infty, \|f\|_L) \leq 1} |\mathbb{E}_x[f(x_{\mathbf{W}})] - \mathbb{E}[f(\sigma Z)]| \leq C' \epsilon$$

A.2 Block Gershgorin Theorem

In Section 3.1, we considered a block diagonal approximation to the Fisher information matrix and derived an upper bound on the spectral norm for all the blocks. Using the properties of the off-diagonal blocks, we can get a more accurate estimate of the maximal eigenvalue of the Fisher information might be. First, let us consider an arbitrarily partitioned matrix $\mathbf{A} \in \mathbb{R}^{N \times N}$, with spectrum $\lambda(\mathbf{A})$. The partitioning is done with respect to the set

$$\pi = \{p_j\}_{j=0}^L \tag{28}$$

with the elements of the set satisfying $0 < p_1 < p_2 < \dots < p_L = N$. Then each block of the matrix $A_{i,j}$ is a potentially rectangular matrix in $\mathbb{R}^{(p_i - p_{i-1}) \times (p_j - p_{j-1})}$. We assume that $\mathbf{A}_{i,i}$ is self-adjoint for all i .

Let us define a disk as

$$C(c, r) \triangleq \{\lambda : \|c - \lambda\| \leq r\}. \tag{29}$$

The theorem as presented in Tretter [33] shows that the eigenvalues of $\lambda(\mathbf{A})$ are contained in a union of Gershgorin disks defined as follows

$$\lambda(\mathbf{A}) \subset \bigcup_{i=1}^L \left\{ \bigcup_{k=1}^{p_i - p_{i-1}} C \left(\lambda_k(\mathbf{A}_{ii}), \sum_{j=1, j \neq i}^L s_{max}(\mathbf{A}_{i,j}) \right) \right\} \tag{30}$$

where the inner union is over a set disks for each eigenvalue of the block diagonal $\mathbf{A}_{i,i}$ while the outer union is over the L blocks in \mathbf{A} . The radius of the disk is constant for every eigenvalue in the i^{th} diagonal block $\mathbf{A}_{i,i}$ and is given by the sum of singular values of the off diagonal blocks. Therefore, the largest eigenvalue of \mathbf{A} lies in

$$\lambda_{max}(\mathbf{A}) \subset \bigcup_{i=1}^L C \left(\lambda_{max}(\mathbf{A}_{ii}), \sum_{j=1, j \neq i}^L s_{max}(\mathbf{A}_{i,j}) \right) \tag{31}$$

We then apply the theorem to the blocks of the Fisher information matrix derived under the conditions mentioned in 3.1. We replace the singular values and eigenvalues with upper bounds given by products of spectral norms of matrices. Similarly, the disc inclusion is replaced by an upper bound. For the bias blocks the upper bound the associated eigenvalue is

$$\max_i \left(\lambda_{max}(\mathbf{H}_g) s_{max}^2(\mathbf{J}_{\mathbf{x}^i}^{\mathbf{x}^L}) + \sum_{j=0, j \neq i}^L \lambda_{max}(\mathbf{H}_g) s_{max}(\mathbf{J}_{\mathbf{x}^i}^{\mathbf{x}^L}) s_{max}(\mathbf{J}_{\mathbf{x}^j}^{\mathbf{x}^L}) \right) \tag{32}$$

where L is the number of hidden layers, while for the weight blocks it is

$$\max_i \left(q^* \lambda_{max}(\mathbf{H}_g) s_{max}^2(\mathbf{J}_{\mathbf{x}^i}^{\mathbf{x}^L}) + \sum_{j=0, j \neq i}^L q^* \lambda_{max}(\mathbf{H}_g) s_{max}(\mathbf{J}_{\mathbf{x}^i}^{\mathbf{x}^L}) s_{max}(\mathbf{J}_{\mathbf{x}^j}^{\mathbf{x}^L}) \right) \tag{33}$$

Again, to simplify this we consider that $s_{max}(\mathbf{J}_{\mathbf{x}^j}^{\mathbf{x}^L})$ monotonically increases as $j \rightarrow 0$ since $s_{max}(\mathbf{J}_{\mathbf{x}^j}^{\mathbf{x}^L})$ appears both in the left and right hand of the summation. Therefore we have that if $q^* > 1$:

$$\lambda_{max}(\bar{\mathbf{G}}) \leq q^* \lambda_{max}(\mathbf{H}_g) s_{max}(\mathbf{J}_{\mathbf{x}^0}^{\mathbf{x}^L}) \left(s_{max}(\mathbf{J}_{\mathbf{x}^0}^{\mathbf{x}^L}) + \sum_{j=1}^L s_{max}(\mathbf{J}_{\mathbf{x}^j}^{\mathbf{x}^L}) \right) \tag{34}$$

if $q^* \leq 1$ we have

$$\lambda_{max}(\bar{\mathbf{G}}) \leq \lambda_{max}(\mathbf{H}_g) s_{max}(\mathbf{J}_{\mathbf{x}^0}^{\mathbf{x}^L}) \left(s_{max}(\mathbf{J}_{\mathbf{x}^0}^{\mathbf{x}^L}) + \sum_{j=1}^L s_{max}(\mathbf{J}_{\mathbf{x}^j}^{\mathbf{x}^L}) \right) \quad (35)$$

The block diagonal approximation considered in Section 3.1 is asymptotically tight if $s_{max}(\mathbf{J}_{\mathbf{x}^0}^{\mathbf{x}^L}) \gg \sum_{j=1}^L s_{max}(\mathbf{J}_{\mathbf{x}^j}^{\mathbf{x}^L})$. Practically this would require that the maximum singular values increase at certain rate as we increase the number of layer through which we backpropagate.